

Environmental Science Processes & Impacts

Accepted Manuscript



This is an *Accepted Manuscript*, which has been through the Royal Society of Chemistry peer review process and has been accepted for publication.

Accepted Manuscripts are published online shortly after acceptance, before technical editing, formatting and proof reading. Using this free service, authors can make their results available to the community, in citable form, before we publish the edited article. We will replace this *Accepted Manuscript* with the edited and formatted *Advance Article* as soon as it is available.

You can find more information about *Accepted Manuscripts* in the [Information for Authors](#).

Please note that technical editing may introduce minor changes to the text and/or graphics, which may alter content. The journal's standard [Terms & Conditions](#) and the [Ethical guidelines](#) still apply. In no event shall the Royal Society of Chemistry be held responsible for any errors or omissions in this *Accepted Manuscript* or any consequences arising from the use of any information it contains.

Benzotriazole corrosion inhibitors are frequently detected in rivers, lakes and groundwater and are not completely removed during wastewater treatment. Photochemical transformation may be a major degradation pathway in the environment. Presented here are kinetic studies and photochemical half-lives under natural conditions for substituted benzotriazoles and a structural series consisting of benzimidazole, indazole, and inole. Benzotriazole undergoes direct photodegradation and reacts rapidly with hydroxyl radicals, but is relatively unreactive towards singlet oxygen. Despite long photochemical half-lives, photochemical transformation may take over a prominent role because little removal by sorption to particles and slow microbial degradation processes are expected in surface water.

26 Abstract

27 Benzotriazole corrosion inhibitors are not completely removed during wastewater
28 treatment and are frequently detected in surface waters. Here, the photochemical
29 kinetics of benzotriazoles and structurally related compounds were assessed for
30 natural aqueous environments. The direct photochemical half-lives during exposure to
31 simulated sunlight ranged from 1.3 to 1.8 days for benzotriazole and its derivatives
32 (4-methyl-, 5-methyl-, 4-hydroxy-substituted benzotriazoles). Benzotriazole is more
33 resistant to direct photodegradation than indazole (0.28 days) and indole (0.09 days),
34 while benzimidazole showed no significant decay. Hydroxyl radicals (1.6×10^{-16} M)
35 and singlet oxygen (2.5×10^{-13} M) are formed during simulated sunlight exposure in
36 the presence of dissolved organic matter ($13 \text{ mg}_C \text{ L}^{-1}$). All tested compounds reacted
37 rapidly with hydroxyl radicals near the diffusion-controlled limit (8.3 to $12 \times 10^9 \text{ M}^{-1}$
38 s^{-1}). Only 4-hydroxybenzotriazole and indole showed significant reactivity towards
39 singlet oxygen and their photochemical half-lives in the presence of organic matter
40 were shorter (0.1 days for both) than for benzotriazole and its methylated derivatives
41 (1.4-1.5 days). The photochemical half-lives determined here are relatively long and
42 support the persistence of benzotriazoles in the environment. At the same time, these
43 results suggest that photochemical transformation can be supplementary to microbial
44 degradation. While the presented study focused on environmental photodegradation
45 kinetics, the relevance of transformation products remains to be investigated.

46

47 **Keywords:** benzimidazole, indazole, indole, organic matter, half-lives

48

49

50 Introduction

51 Quantifying and comparing environmental fate processes of organic pollutants is
52 necessary to determine their persistence in the environment. In 2010, benzotriazole
53 was identified as the fourth most common groundwater pollutant just after bisphenol
54 A with concentrations as high as 100 ng L^{-1} , yet, its environmental persistence and
55 fate processes are not completely understood.¹

56 Benzotriazole and its methylated derivatives (4-methylbenzotriazole and 5-
57 methylbenzotriazole) are widely used anticorrosion agents in airplane deicing fluids
58 and automotive cooling applications.² Other benzotriazole derivatives have been used
59 as ultraviolet light stabilizers in plastics, additives in dishwasher detergent, and
60 chemical intermediates in dyes.^{2,3} Benzotriazole was first detected in the environment
61 in subsurface waters beneath a North American airport.⁴ Diffuse loss of significant
62 amounts (often more than 20%) of deicing fluids after aircraft deicing operations
63 occurs even when collection systems are in place, and these fluids contain
64 approximately 0.05% of benzotriazole if undiluted.⁵ Removal in wastewater treatment
65 plants is incomplete and ranges from 13% to 62% and effluent concentrations are
66 present in the low μM range (4.6 to $10 \mu\text{M}$)^{1, 6-10}. Consequently, benzotriazole has
67 been detected in various lakes, rivers^{3, 7, 8, 11, 12} and groundwater^{1, 4, 13, 14}, and its
68 occurrence and analytic protocols have recently been reviewed by Herrero et al.¹⁵
69 Benzotriazole has also been detected in tap water across Europe up to a concentration
70 of $6.3 \mu\text{g L}^{-1}$.^{3, 13, 16} No specific toxicity of benzotriazole is known but it can cause
71 acute and chronic effects in algae and bacteria and endocrine disrupting effects in fish
72 (Chinese rare minnows) at low mM concentrations.¹⁷⁻¹⁹ Thus, toxic effects may be
73 most pronounced in the winter season when high quantities of deicing fluids are being
74 used and aqueous concentrations increase locally.

75 Benzotriazoles are persistent in the aquatic environment because microbial
76 degradation is slow and removal by sorption and sedimentation is not expected due to
77 its low affinity to organic matter ($\log K_{ow} = 1.23$, $\log K_{oc} = 2.85$).^{2, 14, 20, 21}
78 Consequently, photochemical degradation may be a relevant natural fate process of
79 benzotriazole in surface waters.

80 Many studies have examined the photochemistry of benzotriazole under enhanced
81 UVC light conditions (254 nm), focusing on degradation mechanism and kinetics.
82 Different photoproducts, such as aniline and phenazine, were identified and laser flash
83 photolysis demonstrated that the five-member ring was broken from an N-N bond
84 fission with high-energy irradiation.^{22, 23} Several studies have confirmed that the
85 photodegradation of benzotriazole is pH-dependent (pK_a around 8.6)²³⁻²⁵ with faster
86 decay at lower pH as the deprotonated species is much less photoreactive due to lower
87 absorptivity.²⁴ During irradiation with UVC light (254 nm), the decay rates were
88 slower in the presence of organic matter, which was assumed to be due to light
89 screening and scavenging of hydroxyl radicals ($\cdot OH$) by the organic matter.^{25, 26}
90 While these studies offer information for engineered systems such as advanced
91 drinking water and wastewater treatment, they are not representative for fate
92 processes under natural conditions in the environment. In the aquatic environment,
93 organic matter acts as a photosensitizer due to production of excited organic matter
94 itself and reactive oxygen species (e.g., singlet oxygen and hydroxyl radicals). In
95 addition to transformation of benzotriazoles by direct photochemical processes
96 indirect photochemical reactions with these organic matter-derived reactive species
97 have yet to be quantified.

98 The present study focuses on photochemical degradation kinetics of
99 benzotriazole derivatives but also includes the structurally related compounds

100 benzimidazole, indazole and indole. The environmental fate of benzimidazole has not
101 been studied in detail with the exception of carbendazim,²⁷⁻²⁹ a benzimidazole
102 derivative. Due to its presence in a wide range of pesticides and pharmaceuticals,
103 benzimidazole is likely to be found in the aquatic environment.^{28, 30} Monitoring the
104 persistence of benzimidazole fungicides in surface waters is necessary, as they can
105 cause toxic effects in aquatic microorganisms and invertebrates.³¹

106 Here, we identified photochemical transformation processes of benzotriazole and
107 structurally related compounds to investigate their fate processes in the aquatic
108 environment. We assessed the half-lives for direct photodegradation, the reactivity
109 with reactive oxygen species (hydroxyl radicals, singlet oxygen), and the effects of
110 organic matter on the transformation kinetics of these compounds during light
111 exposure. We demonstrated that benzotriazole undergoes direct photodegradation by
112 UVB irradiation and reacts rapidly with hydroxyl radicals, but is relatively unreactive
113 towards singlet oxygen. Overall, our results suggest that the fate by photochemical
114 processes is competitive with microbial degradation in surface waters.

115

116 **Materials and Methods**

117 **Materials.** All solutions were prepared with nanopure water (resistivity > 18 MΩ
118 cm, Barnstead NANOpure System). Experiments at pH 7.5 were carried out in 10
119 mM phosphate buffer from sodium phosphate dibasic dihydrate (Sigma Aldrich, ≥
120 99%) adjusted to 30 mM ionic strength with sodium chloride (Merck, ACD reagent
121 grade). The following reagents were used as received: Indole (Sigma Aldrich, 99+%),
122 indazole (Sigma Aldrich, 98%), benzimidazole (Sigma Aldrich, 98%), benzotriazole
123 (TCI, >98.0%), 4-methylbenzotriazole (Fluka), 5-methylbenzotriazole (Acros
124 organics), 4-hydroxybenzotriazole (Aldrich), 2-hydroxyterephthalic acid (Sigma

125 Aldrich, 97%); Rose Bengal (Sigma-Aldrich), p-nitroanisole (Aldrich), pyridine
126 (Sigma), ammonium bicarbonate (Fluka), ammonium acetate (Prolabo®), formic acid
127 (AnalaR NORMAPUR VWR, 99-100%), acetic acid (Fluka), and ethanol (Fluka);
128 acetonitrile and methanol (Merck KGaA, ≥ 99.9). Furfuryl alcohol (Aldrich) was
129 distilled prior to use. The terephthalic acid potassium salt (K_2 TPA) was prepared from
130 terephthalic acid (Sigma Aldrich, 98%) as described elsewhere.³² Briefly, TPA (0.06
131 moles) and KOH (0.12 moles) were dissolved in nanopure water, placed on ice, and
132 ethanol was added to precipitate a white powder. The precipitate (K_2 TPA) was
133 filtered and dried on a vacuum line for 90 minutes.

134 Stock solutions of the test compounds were prepared daily in nanopure water.
135 Suwannee River Fulvic Acid II (SRFA II, 1S101F) and Waskish Peat organic matter
136 (1R107H) were obtained from the International Humic Substances Society (IHSS)
137 (St. Paul, MN, USA) and solutions were prepared by dissolving approximately 250
138 $mg_{HA} L^{-1}$ in nanopure water at pH 10.0 by adding sodium hydroxide and sonicating
139 the solutions until a stable pH was reached. DOM solutions were then adjusted to
140 around pH 7 with hydrochloric acid, filter sterilized (0.2 μm , cellulose acetate
141 membrane, VWR), and frozen until use. The total organic carbon content was
142 determined (Shimadzu Corporation, TOC-L analyzer).

143

144 **Photodegradation during light exposure**

145 Solutions of test compounds (10 μM) were exposed to light from a Xe lamp
146 (Newport, at 300 W, see Figure 1A for spectrum) simulating the solar light spectrum
147 with and without dissolved organic matter (SRFA(II), 13 $mg_C L^{-1}$) present. For
148 exposure to enhanced UVB or UVA light, a photoreactor (Rayonet; Southern New

149 England Ultraviolet Co, see supporting information (SI), **Figure S1** for spectra) with
150 six RPR-3000 Å or eight RPR-3500 Å bulbs, respectively, was used.

151 All test solutions contained furfuryl alcohol (40 µM) as a singlet oxygen probe
152 molecule. Solutions (4 mL) were placed into borosilicate tubes (PYREX®, 7.5 cm,
153 inner diameter 1.0 cm) in front of the Xe Lamp and stirred (400 rpm). The steady
154 state hydroxyl radical concentration ($[\cdot\text{OH}]_{\text{ss}}$) was quantified using TPA as a hydroxyl
155 radical probe molecule for experiments in the sunlight simulator with organic matter
156 (SRFA(II)). TPA reacts with hydroxyl radical to give a hydroxylated fluorescent
157 product, hydroxyterephthalic acid (hTPA)³². To determine $[\cdot\text{OH}]_{\text{ss}}$ a solution in an
158 open borosilicate tube (PYREX®, 8.5 cm, inner diameter 1.5 cm) containing
159 SRFA(II) (13 mg_C L⁻¹) and TPA potassium salt (10 µM) was irradiated under the
160 same conditions as applied in the sunlight simulator experiments (Xe lamp, Newport,
161 at 300 W). The $[\cdot\text{OH}]_{\text{ss}}$ was calculated by monitoring the production of hTPA (**SI**,
162 **Figure S2**). The production rate constant of hTPA was divided by (a) the average
163 percent yield of 35% for hTPA produced by the reaction of TPA and hydroxyl
164 radical,³² (b) by the concentration of TPA (10 µM), and (b) by the second order
165 reaction rate constant of TPA with hydroxyl radical ($4.4 \times 10^9 \text{ M}^{-1} \text{ s}^{-1}$).³² The $[\cdot\text{OH}]_{\text{ss}}$
166 produced from SRFA(II) during sunlight simulator experiments was calculated as 1.6
167 $\pm 0.1 \times 10^{-16} \text{ M}$.

168 To calculate the quantum yields for direct photolysis, analogous experiments were
169 performed in enhanced UVB light (Rayonet with eight RPR-3000 Å bulbs). The
170 spectral overlap of the UVB light source and the absorption of the compounds were
171 higher than for the Xe-lamp, which reduces the error in these calculations. A p-
172 nitroanisole-pyridine actinometer was used³³. Therefore, solutions of p-nitroanisole (8
173 µM) and pyridine (0.5 mM) in nanopure water were irradiated in quartz tubes.

174 Details on the degradation kinetics of p-nitroanisole and test compounds and the
175 quantum yield calculation can be found in the SI (Figure S3, Table S1-S2).

176 **Reaction rate constants with reactive oxygen species**

177 *Singlet oxygen.* The reaction rate constant with singlet oxygen was measured in
178 solutions containing sensitizer (Rose Bengal, 1-10 μM), furfuryl alcohol (40 μM) and
179 the test compound (10 μM) at pH 7.5, irradiated by a Xe lamp (Newport, at 300 W,
180 455 nm low pass filter) while stirred in borosilicate tubes. Rose Bengal photobleached
181 during extended light exposure. For the compounds that required longer exposure
182 time because of their low reactivity, the concentration of Rose Bengal was quantified
183 spectroscopically every 30 minutes and re-adjusted to maintain constant
184 concentrations throughout the experiment. The steady-state singlet oxygen
185 concentration, $[^1\text{O}_2]_{\text{ss}}$, was assessed by dividing the observed degradation rate
186 constants (k_{obs} , s^{-1}) of furfuryl alcohol by its second order reaction rate constant of 8.3
187 $\pm 0.1 \times 10^7 \text{ M}^{-1} \text{ s}^{-1}$.³⁴ The second order reaction rate constant of the test compounds
188 were then assessed by dividing their observed decay rate constants (k_{obs} , s^{-1}) by
189 $[^1\text{O}_2]_{\text{ss}}$.

190 *Hydroxyl radicals.* The degradation rate constants from the reaction with hydroxyl
191 radical were assessed by competitive kinetics studies with benzoic acid. Reaction
192 solutions prepared in nanopure water consisted of benzoic acid (5 μM), test
193 compound (5 μM), and 1 mM hydrogen peroxide (H_2O_2) to produce hydroxyl radical
194 during exposure to UVA light. Solutions (4 mL) were placed into borosilicate tubes
195 (PYREX®, 7.5 cm, inner diameter 1.0 cm) on a turntable inside a photoreactor
196 (Rayonet; Southern New England Ultraviolet Co, eight RPR-3650 Å bulbs). None of
197 the test compounds of interest absorb light at 365 nm and no degradation by direct
198 photochemical reactions was observed. The second order reaction rate constants of

199 the test compounds with hydroxyl radical were determined by linear regression of the
200 degradation of test compound (as $\ln[C/C_0]$) versus the degradation of benzoic acid (as
201 $\ln[C/C_0]$) and the corresponding slope was multiplied by the reaction rate constant of
202 benzoic acid with hydroxyl radical, $5.9 \times 10^9 \text{ M}^{-1} \text{ s}^{-1}$.³⁵

203

204 **Sample analysis**

205 Samples were analyzed by Ultra Performance Liquid Chromatography
206 (UPLC) on a C18 column (Waters Aquity, BEH130 C18, 1.7 μm , 2.1 \times 150 mm) with
207 injection volume of 5 μL . Furfuryl alcohol and all test compounds were analyzed
208 using 75% sodium acetate buffer (pH 5.9, 15.6 mM) and 25% acetonitrile with 0.15
209 ml min^{-1} flow rate. Furfuryl alcohol was detected by absorbance at 219 nm.
210 Benzotriazole, 4-methylbenzotriazole and 5-methylbenzotriazole were detected by
211 absorbance at 275 nm and 4-hydroxybenzotriazole was detected by absorbance at 290
212 nm. Benzimidazole, indazole and indole were detected by fluorescence with
213 excitation at 275 nm and emission at 320, 315, and 350 nm, respectively. The
214 analysis of benzoic acid was performed on the same UPLC with a using formic acid
215 (0.1%) and methanol (B) with the following gradient: 0-3 min, 85%A-15%B; 3-8
216 min, 50%A-50%B; 8-10 min, 0%A-100%B; 10-15 min 85%A-15%B followed by
217 fluorescence detection with excitation at 225 nm and emission at 425 nm. For
218 hydroxyterephthalate, an eluent composition of 70% formic acid (0.1%) and 30%
219 methanol and fluorescence detection with excitation at 250 nm and emission at 410
220 nm was used. For p-nitroanisole, an eluent composition of 40% acetate buffer (pH
221 5.0, 15.6 mM) and 60% acetonitrile and absorbance detection at 316 nm was used.

222 All first-order degradation rate constants, k_{obs} (s^{-1}), were assessed by linear
223 regression of normalized, log-transformed normalized concentrations ($\ln(C/C_0)$)
224 versus irradiation time.

225

226 **Results and Discussion**

227 The photochemical degradation kinetics of benzotriazole derivatives and
228 structurally related compounds are presented below. We first present the degradation
229 kinetics and half-lives under simulated sunlight conditions for direct photochemical
230 processes. Then we quantify the reaction rate constants with hydroxyl radicals and
231 singlet oxygen. Finally, we show the effects of DOM and assess the contribution of
232 indirect processes to the overall photochemical half-lives.

233 In addition to benzotriazole derivatives, we also investigated the structurally
234 related compounds benzimidazole, indole, and indazole, which differ in the number
235 and position of the N atoms in the 5-membered ring (see Figure 1B for structures).
236 Some benzimidazole fungicides (e.g., 2-aminobenzimidazole and carbendazim) have
237 been detected in secondary wastewater treatment plant effluent, emphasizing the
238 stability of benzimidazole and its occurrence in surface water.^{28, 36-38} However,
239 indirect photochemical reactivity of benzimidazole in the presence of organic matter
240 has not yet been studied. Indazoles are rare in nature but are often part of the structure
241 of biologically active compounds.³⁹ Lastly, indole is the backbone of a wide variety of
242 naturally occurring biomolecules, including tryptophan, an essential amino acid.⁴⁰ We
243 studied these compounds to further investigate possible structural effects of nitrogen-
244 heterocyclic compounds on photodegradation relative to benzotriazoles and to assess
245 the connection between the photochemistry of benzotriazoles and the indole-
246 containing amino acid tryptophan.⁴¹

247

248 **Photodegradation and half-lives**

249 Benzotriazoles and structurally related compounds undergo direct photochemical
250 reactions because they absorb light in the UVB range of the solar spectrum, with the
251 exception of benzimidazole (**Figure 1**). Benzimidazole was also one of the
252 photoproducts identified for photodegradation of carbendazim²⁹ and is thus expected
253 to be relatively photostable. Data in **Figure 2** show direct photochemical degradation
254 of the tested compounds during exposure to simulated sunlight. Indole and indazole
255 degrade significantly faster with half-lives of 0.1 and 0.3 days, respectively, compared
256 to benzotriazole (1.8 days). The methylated and hydroxylated benzotriazole
257 derivatives all decay at similar rates with half-lives ranging from 1.3 to 1.6 days
258 (**Table 1**). To calculate quantum yields for direct photochemical degradation,
259 analogous experiments were performed in enhanced UVB light (see SI for details).
260 Benzotriazole shows similar molar absorptivity as indole and indazole, yet a lower
261 quantum yield results in the slower observed degradation kinetics.

262 For benzotriazole, direct photochemical transformation may lead to opening of the
263 five-member ring from a N-N bond fission as observed previously with high-energy
264 irradiation.^{22, 23} Future research should further investigate the identification and
265 quantification of photoproducts of benzotriazole under sunlight conditions.

266 **Effects of reactive oxygen species and organic matter.** Dissolved organic matter
267 can act as a sensitizer and thus enhance degradation of organic molecules by indirect
268 photochemical processes. Here, we investigated the reactivity of all test compounds
269 with hydroxyl radicals and singlet oxygen. The data show that these are the two
270 prominent reactive oxygen species contributing to the indirect photodegradation of
271 benzotriazole derivatives and structurally related compounds.

272 **Hydroxyl radicals.** The reaction rate constants of all test compounds have been
273 assessed by competitive reaction of benzoic acid with hydroxyl radical, which was
274 produced photochemically from hydrogen peroxide (for kinetic data see SI, **Figure S4**
275 **and Figure S5**). All compounds are reactive towards hydroxyl radical with reaction
276 rate constants near the diffusion-controlled limit (**Table 1**). The reaction with
277 hydroxyl radical is expected to include radical addition reactions resulting in
278 hydroxylation of the benzene ring. Formation of 4-hydroxybenzotriazole was
279 observed in analogous experiment with higher starting concentration of benzotriazole
280 (50 μM , **Figure S6**, **Figure S7**). The yield of 4-hydroxybenzotriazole formation was
281 relatively low ($\sim 4\%$). Methylated and hydroxylated benzotriazoles reacted slightly
282 faster than unsubstituted benzotriazole, likely due to the increased the electron density
283 in the benzene ring from the electron donating methyl and hydroxy substituents.
284 Steady-state concentrations of hydroxyl radicals in surface waters are relatively low
285 ranging from 10^{-15} to 10^{-17} M.^{42,43} Thus, despite the high reactivity, the reaction with
286 hydroxyl radicals may cause only moderate transformation of benzotriazole
287 derivatives in the environment.

288 **Singlet oxygen.** Data in **Table 1** also show the reaction rate constants of singlet
289 oxygen with all test compounds (further information in SI, **Table S3**). Among all test
290 compounds, only 4-hydroxybenzotriazole and indole react at relatively fast rates with
291 singlet oxygen ($k = 1.31 \pm 0.04 \times 10^8 \text{ M}^{-1} \text{ s}^{-1}$ and $k = 4.34 \pm 0.01 \times 10^7 \text{ M}^{-1} \text{ s}^{-1}$,
292 respectively). The reaction rate constant of 4-hydroxybenzotriazole represents the
293 combined rate constants of the phenol and phenolate species ($\text{pK}_a = 7.7$, experimental
294 $\text{pH} = 7.5$). The reaction of singlet oxygen with other benzotriazole derivatives are so
295 slow ($k < 6.0 \times 10^5 \text{ M}^{-1} \text{ s}^{-1}$) that the reaction is not expected to contribute significantly

296 to their fate in the environment, considering environmental steady-state
297 concentrations of singlet oxygen of 10^{-12} to 10^{-13} M in surface waters.⁴⁴⁻⁴⁶

298 Comparing indole to indazole and benzimidazole, the additional nitrogen in the 5-
299 membered ring may be the cause of lower reactivity of indazole and benzimidazole
300 with singlet oxygen. Indoles are thought to react with singlet oxygen at the 2,3-C=C
301 double bond and substitution with N atoms at the 2-position (indazole), 3-position
302 (benzimidazole) or both positions (benzotriazole) disrupts this site of attack. It is
303 notable that histidine carries the same imidazole ring structure as benzimidazole and
304 reacts rapidly with singlet oxygen ($k = 8.3 \pm 1.1 \times 10^7 \text{ M}^{-1} \text{ s}^{-1}$).⁴⁷ Imidazoles react
305 with singlet oxygen across the 2,4 (or 2,5) C atoms. This mode of reactivity is not
306 favored for benzimidazole because it would lead to disruption of aromaticity in the
307 adjoining ring.

308 ***Dissolved organic matter.*** Data in **Figure 3A** show that the decay of benzotriazole
309 only increases slightly in the presence of $13 \text{ mg}_C \text{ L}^{-1}$ of Suwannee River Fulvic Acid
310 (II) during exposure to simulated sunlight and after correcting for light screening
311 effects (Student t-test, $p < 0.001$). The observed half-life was 1.4 days and represents
312 transformation by direct and indirect photochemical processes. Enhanced degradation
313 can be attributed to the reaction with hydroxyl radicals. We measured the steady-state
314 concentration of hydroxyl radicals to be $1.6 \times 10^{-16} \text{ M}$ during exposure of DOM
315 (SRFA(II), $13 \text{ mg}_C \text{ L}^{-1}$) to simulated sunlight. The estimated half-life based on the
316 reaction with this concentration of hydroxyl radicals was 5.8 days.

317 Previous studies reported a net inhibition effect of DOM on the degradation of
318 benzotriazole.²⁵ Data in **Figure 3B** demonstrate that light screening is mostly
319 responsible for these observations. The decay rate of benzotriazole progressively
320 decreases with increasing concentration of DOM during exposure to enhanced UVB

321 light. The sensitizing effect of DOM increases with DOM (sensitizer) concentration
322 and only becomes apparent after correcting for light screening (see SI **Table S4** for
323 details).

324 Data in **Figure 4** summarize the reaction rate constants during exposure to
325 simulated sunlight and data in **Table 1** shows the photochemical half-lives that were
326 observed in the presence and absence of DOM. The last column in **Table 1** lists half-
327 lives based on the reactions with hydroxyl radicals and singlet oxygen as estimated
328 from the compound-specific reaction rate constants and the steady-state
329 concentrations of the reactive oxygen species.

330 The presence of DOM had minimal effects on benzotriazole and its methylated
331 derivatives. The observed indirect photochemical decay in the presence of DOM
332 (**Figure 4**, dark grey bars) is well described by the sum of direct degradation rates and
333 the estimated reaction rate with hydroxyl radical (stacked bars). This is also true for
334 indazole and benzimidazole. In contrast, DOM significantly sensitized the
335 degradation of 4-hydroxybenzotriazole, decreasing the photochemical half-life from
336 1.3 days ('no DOM') to 0.1 days ('with DOM'). However, the reaction with hydroxyl
337 radical and singlet oxygen alone cannot explain the observed enhancement. We
338 believe the discrepancy is due to reactivity with triplet-state DOM. Excited-state
339 DOM can oxidize organic molecules by direct electron abstraction or via an energy
340 transfer pathway^{48, 49} and may be the reason for the enhanced reactivity of 4-
341 hydroxybenzotriazole.

342 Indole degrades rapidly during irradiation with a half-life of 0.7 days and the
343 reaction with singlet oxygen accounts for the majority of indirect photochemical
344 degradation. The observed decay rate in the presence of DOM is 30% lower than the
345 estimated decay rate based on direct transformation and the estimated reaction rate

346 constant with singlet oxygen and hydroxyl radicals. This difference can be explained
347 by the fact that dissolved organic matter does not only sensitize but also slows down
348 the photochemical decay of indole by repairing photodamage. Previous studies show
349 that an indole radical cation is formed by direct photochemical reactions of indole and
350 that in the case of tryptophan, this indole radical cation can be reduced back to indole
351 by electron donors present in DOM.^{41, 50} The fact that this non-screening inhibition
352 behavior was not observed for benzotriazole derivatives suggests that they do not
353 undergo photoionization as indole does, presumably due to their higher ionization
354 energies.

355

356 **Conclusions.**

357 The presented data suggest that DOM is a net sensitizer in sunlit aqueous
358 environments for the degradation of benzotriazole and structurally related compounds
359 (with the exception of indole). Despite the structural similarity of benzotriazole to the
360 highly photoreactive indole, it is much less photoreactive. In the top layer of sunlit
361 surface waters, these benzotriazole derivatives are expected to naturally decay by
362 direct photochemical processes. However, the photochemical half-lives are relatively
363 long (1.3-1.8 days), supporting the persistence of benzotriazoles in the environment.
364 Below the water surface where UV light is progressively screened, DOM still acts as
365 a sensitizer and indirect phototransformation of benzotriazoles by reaction with
366 hydroxyl radicals could become relatively more important. 4-Hydroxybenzotriazole
367 is a product of photochemical and microbial transformation of benzotriazole.¹⁰ The
368 high photochemical reactivity of 4-hydroxybenzotriazole observed here suggests that
369 it is not a stable end-product in the sunlit aquatic environment.

370 Despite the long photochemical half-lives, photochemical transformation appears
371 to be a significant degradation process in the aquatic environment because removal by
372 sorption to particles and microbial degradation processes are slow.^{2, 14, 20, 21} Measured
373 biodegradation half-lives of benzotriazole and 5-methylbenzotriazole for the decay
374 during wastewater treatment are 1.0 and 0.9 days, respectively¹⁰. In particular, 4-
375 methylbenzotriazole is more stable in wastewater treatment (half-life of 8.5 days)^{7, 51}
376 Microbial degradation alone is not sufficient to remove benzotriazoles considering the
377 relatively short residence times in a treatment plant (0.5-0.7 days)¹⁰ and much lower
378 microbial activity in surface waters. Once the benzotriazoles entered surface waters,
379 photochemical degradation may take over a prominent role in their transformation.
380 However, the photochemical half-lives are expressed as days of full sunlight exposure
381 and have to be corrected for actual hours of sunlight and sunlight intensity of the date
382 and location of interest, which likely increase reported photochemical half-lives by a
383 factor of five to ten.

384 Despite long half-lives of microbial and photochemical degradation of
385 benzotriazoles, these processes are believed to be the dominant transformation
386 reactions of these otherwise persistent pollutants. With a better understanding of the
387 phototransformation pathways and rates of benzotriazoles, future research should be
388 directed to identify photoproducts and investigate their potential toxic effects relative
389 to the parent compounds.

390

391 **Associated content**

392 Supporting Information. Detailed methodology, Tables S1-S4, and Figures S1-S8.

393

394 **Acknowledgements**

395 We gratefully acknowledge support of the Swiss National Science Foundation (Grant
396 number 200021-138008) for funding and Jeroen van den Wildenberg for assisting
397 with laboratory experiments.

398 **References**

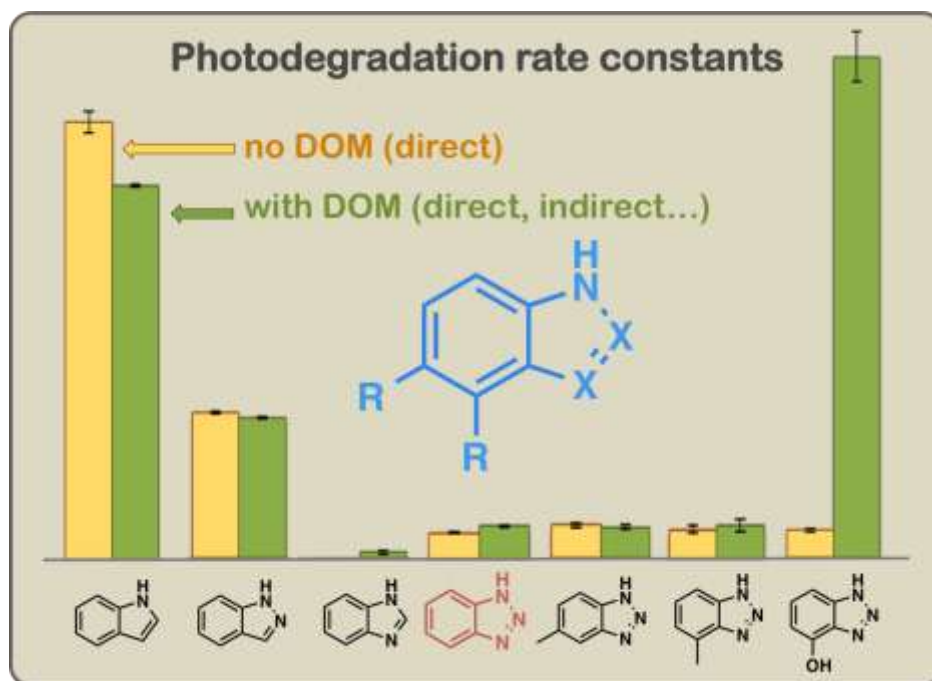
- 399 1. R. Loos, G. Locoro, S. Comero, S. Contini, D. Schwesig, F. Werres, P. Balsaa,
400 O. Gans, S. Weiss, L. Blaha, M. Bolchi and B. M. Gawlik, *Water Research*,
401 2010, 44, 4115-4126.
- 402 2. D. S. Hart, L. C. Davis, L. E. Erickson and T. M. Callender, *Microchemical*
403 *Journal*, 2004, 77, 9-17.
- 404 3. W. Giger, C. Schaffner and H. P. E. Kohler, *Environmental Science &*
405 *Technology*, 2006, 40, 7186-7192.
- 406 4. D. A. Cancilla, J. Martinez and G. C. van Aggelen, *Environmental Science &*
407 *Technology*, 1998, 32, 3834-3835.
- 408 5. G. D. Breedveld, R. Roseth, L. J. Hem and M. Sparrevik, *Triazoles in the*
409 *terrestrial environment*, Norwegian Geotechnical Institute, Aquateam,
410 Jordforsk, 2002.
- 411 6. D. Voutsas, P. Hartmann, C. Schaffner and W. Giger, *Environ Sci Pollut R*,
412 2006, 13, 333-341.
- 413 7. S. Weiss, J. Jakobs and T. Reemtsma, *Environmental Science & Technology*,
414 2006, 40, 7193-7199.
- 415 8. T. Reemtsma, U. Miehe, U. Duennbier and M. Jekel, *Water Research*, 2010,
416 44, 596-604.
- 417 9. S. D. Richardson and T. A. Ternes, *Anal Chem*, 2011, 83, 4614-4648.
- 418 10. S. Huntscha, T. B. Hofstetter, E. L. Schymanski, S. Spahr and J. Hollender,
419 *Environmental Science & Technology*, 2014, DOI: 10.1021/es405694z.
- 420 11. A. Kiss and E. Fries, *Environ Sci Pollut R*, 2009, 16, 702-710.
- 421 12. R. Loos, B. M. Gawlik, G. Locoro, E. Rimaviciute, S. Contini and G. Bidoglio,
422 *Environ Pollut*, 2009, 157, 561-568.
- 423 13. G. Breedveld, R. Roseth, M. Sparrevik, T. Hartnik and L. Hem, *Water, Air, &*
424 *Soil Pollution: Focus*, 2003, 3, 91-101.
- 425 14. G. D. Breedveld, R. Roseth, L. J. Hem and M. Sparrevik, *Triazoles in the*
426 *terrestrial environment, Final Report*, Report 20001103-1, Norwegian
427 Geotechnical Institute, Oslo, Norway, 2002.
- 428 15. P. Herrero, F. Borrull, E. Pocurull and R. M. Marce, *Trac-Trend Anal Chem*,
429 2014, 62, 46-55.
- 430 16. H. Janna, M. D. Scrimshaw, R. J. Williams, J. Churchley and J. P. Sumpter,
431 *Environmental Science & Technology*, 2011, 45, 3858-3864.
- 432 17. A. Seeland, M. Oetken, A. Kiss, E. Fries and J. Oehlmann, *Environ Sci Pollut*
433 *R*, 2012, 19, 1781-1790.
- 434 18. D. A. Pillard, J. S. Cornell, D. L. Dufresne and M. T. Hernandez, *Water*
435 *Research*, 2001, 35, 557-560.
- 436 19. X. F. Liang, M. Wang, X. Chen, J. M. Zha, H. H. Chen, L. F. Zhu and Z. J. Wang,
437 *Chemosphere*, 2014, 112, 154-162.
- 438 20. C. L. Gruden, S. M. Dow and M. T. Hernandez, *Water Environ Res*, 2001, 73,
439 72-79.
- 440 21. Chemspider, CSID:106892, [http://www.chemspider.com/Chemical-](http://www.chemspider.com/Chemical-Structure.106892.html)
441 [Structure.106892.html](http://www.chemspider.com/Chemical-Structure.106892.html) (accessed 09:53, Jan 6, 2015).
- 442 22. H. Wang, C. Burda, G. Persy and J. Wirz, *Journal of the American Chemical*
443 *Society*, 2000, 122, 5849-5855.
- 444 23. L. J. Hem, T. Hartnik, R. Roseth and G. D. Breedveld, *Journal of*
445 *Environmental Science and Health, Part A*, 2003, 38, 471-481.

- 446 24. R. Andreozzi, V. Caprio, A. Insola and G. Longo, *Journal of Chemical*
447 *Technology & Biotechnology*, 1998, 73, 93-98.
- 448 25. Y.-S. Liu, G.-G. Ying, A. Shareef and R. S. Kookana, *Environmental*
449 *Chemistry*, 2011, 8, 174-181.
- 450 26. F. J. Benitez, J. L. Acero, F. J. Real, G. Roldan and E. Rodriguez, *Journal of*
451 *Environmental Science and Health, Part A*, 2012, 48, 120-128.
- 452 27. A. Boudina, C. Emmelin, A. Baaliouamer, M. F. Grenier-Loustalot and J. M.
453 Chovelon, *Chemosphere*, 2003, 50, 649-655.
- 454 28. J. P. Escalada, A. Pajares, J. Gianotti, W. A. Massad, S. Bertolotti, F. Amat-
455 Guerri and N. A. García, *Chemosphere*, 2006, 65, 237-244.
- 456 29. A. Kiss and D. Virág, *Journal of environmental quality*, 2009, 38, 157-163.
- 457 30. A. A. Spasov, I. N. Yozhitsa, L. I. Bugaeva and V. A. Anisimova, *Pharm Chem*
458 *J*, 1999, 33, 232-243.
- 459 31. S. J. Oh, J. Park, M. J. Lee, S. Y. Park, J.-H. Lee and K. Choi, *Environmental*
460 *Toxicology and Chemistry*, 2006, 25, 2221-2226.
- 461 32. S. E. Page, W. A. Arnold and K. McNeill, *Journal of Environmental*
462 *Monitoring*, 2010, 12, 1658-1665.
- 463 33. A. Leifer, *The Kinetics of Environmental Aquatic Photochemistry*, American
464 Chemical Society, York, PA, 1988.
- 465 34. D. E. Latch, B. L. Stender, J. L. Packer, W. A. Arnold and K. McNeill, *Environ*
466 *Sci Technol*, 2003, 37, 3342-3350.
- 467 35. G. V. Buxton, C. L. Greenstock, W. P. Helman and A. B. Ross, *Journal of*
468 *Physical and Chemical Reference Data*, 1988, 17, 513-886.
- 469 36. J. Hollender, S. G. Zimmermann, S. Koepke, M. Krauss, C. S. McArdell, C.
470 Ort, H. Singer, U. von Gunten and H. Siegrist, *Environmental Science &*
471 *Technology*, 2009, 43, 7862-7869.
- 472 37. G. Palma, A. Sánchez, Y. Olave, F. Encina, R. Palma and R. Barra,
473 *Chemosphere*, 2004, 57, 763-770.
- 474 38. J. W. Readman, T. A. Albanis, D. Barcelo, S. Galassi, J. Tronczynski and G. P.
475 Gabrielides, *Marine Pollution Bulletin*, 1997, 34, 259-263.
- 476 39. A. Schmidt, A. Beutler and B. Snovydovych, *European Journal of Organic*
477 *Chemistry*, 2008, 2008, 4073-4095.
- 478 40. R. B. Van Order and H. G. Lindwall, *Chemical Reviews*, 1942, 30, 69-96.
- 479 41. E. M. L. Janssen, P. R. Erickson and K. McNeill, *Environmental Science &*
480 *Technology*, 2014, DOI: 10.1021/es500535a.
- 481 42. P. L. Brezonik and J. Fulkerson-Brekken, *Environmental Science &*
482 *Technology*, 1998, 32, 3004-3010.
- 483 43. R. G. Zepp, J. Hoigne and H. Bader, *Environmental Science & Technology*,
484 1987, 21, 443-450.
- 485 44. R. G. Zepp, N. L. Wolfe, G. L. Baughman and R. C. Hollis, *Nature*, 1977, 267,
486 421-423.
- 487 45. L. Y. Wick, K. McNeill, M. Rojo, E. Medilanski and P. M. Gschwend,
488 *Environmental Science & Technology*, 2000, 34, 4354-4362.
- 489 46. C. W. Shao, W. J. Cooper and D. R. S. Lean, *Aquatic and Surface*
490 *Photochemistry*, 1994, 215-221.
- 491 47. A. L. Boreen, B. L. Edhlund, J. B. Cotner and K. McNeill, *Environ. Sci.*
492 *Technol.*, 2008, 42, 5492-5498.
- 493 48. R. G. Zepp, P. F. Schlotzhauer and R. M. Sink, *Environmental Science &*
494 *Technology*, 1985, 19, 74-81.

- 495 49. S. Canonica, *Chimia*, 2007, 61, 641-644.
496 50. E. M. Evleth, O. Chalvet and P. Bamiere, *The Journal of Physical Chemistry*,
497 1977, 81, 1913-1917.
498 51. S. Weiss and T. Reemtsma, *Anal Chem*, 2005, 77, 7415-7420.
499
500
501

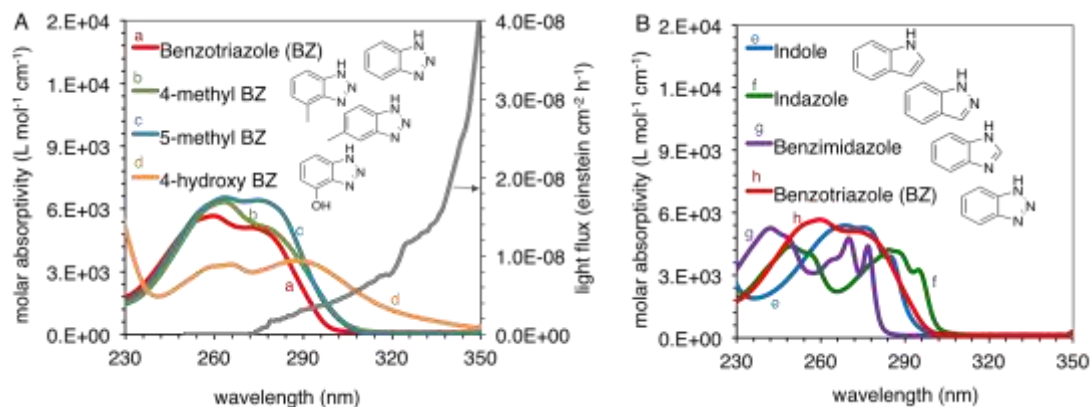
502 Table of Content Art

503



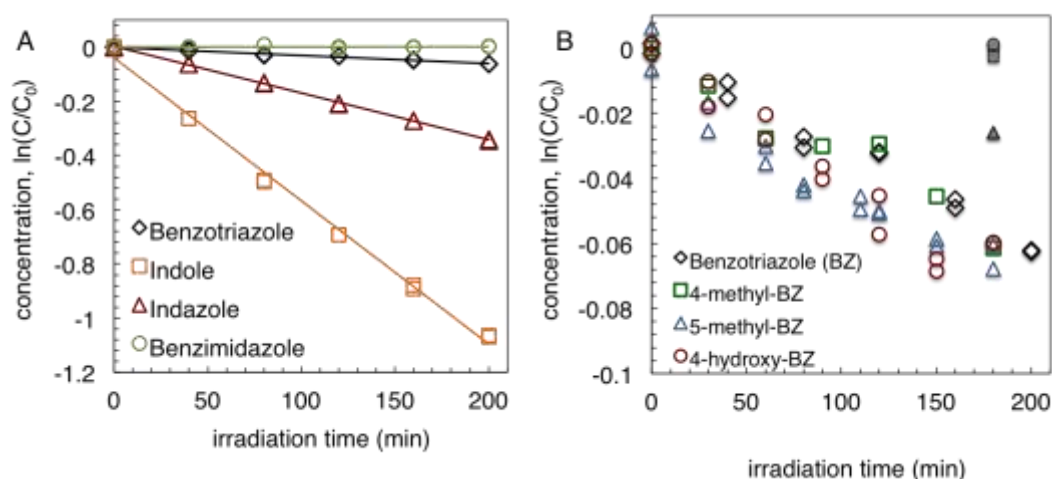
504

505



506

507 **Figure 1.** (A) Light flux of simulated sunlight (Xe-lamp, grey line) and molar
508 absorptivities and chemical structures of benzotriazole derivatives and (B) of indole,
509 indazole, benzimidazole and benzotriazole.



510

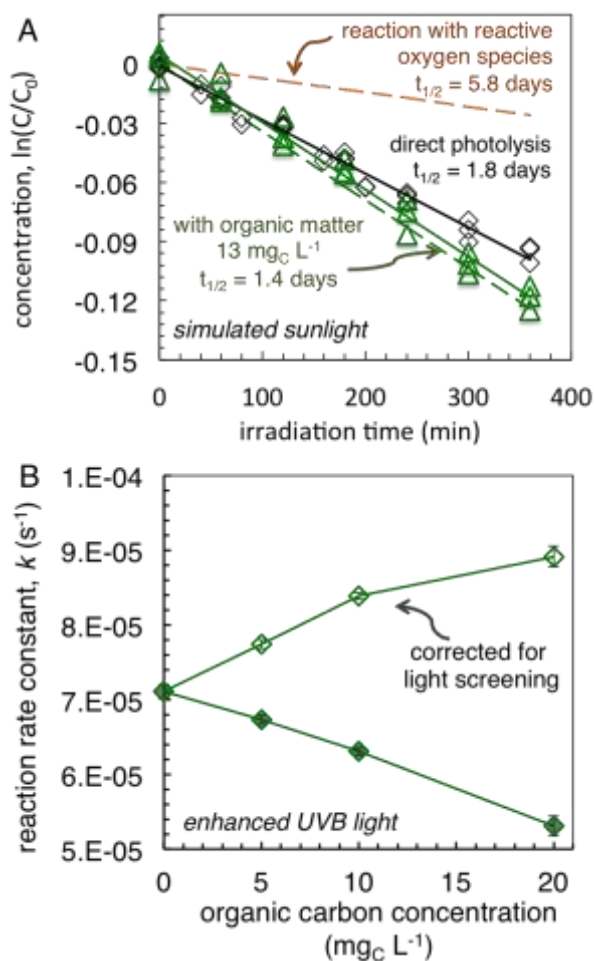
511 **Figure 2.** Degradation during exposure to simulated sunlight for (A) benzimidazole
512 (green circles), benzotriazole (black diamonds), indazole (red triangles), and indole
513 (orange squares) and (B) the benzotriazole derivatives 4-methylbenzotriazole (green
514 squares), 5-methylbenzotriazole (blue triangles) and 4-hydroxybenzotriazole (red
515 circles) and dark control samples (grey symbols). Measurements were performed in
516 duplicate.

517

518

519

520



521

522

523 **Figure 3.** (A) Degradation of benzotriazole during exposure to simulated sunlight

524 (black diamonds) and in the presence of organic matter (green triangles, SRFA(II), 13

525 mg_C L⁻¹), solid lines represented linear regression of measured data, dashed lines

526 represent estimated degradation for the reaction with hydroxyl radical and singlet

527 oxygen (orange dashed line) and the sum of direct and indirect reactions in the

528 presence of organic matter (green dashed line). Data is corrected for light screening

529 effects. (B) Reaction rate constants of benzotriazole during exposure to enhanced

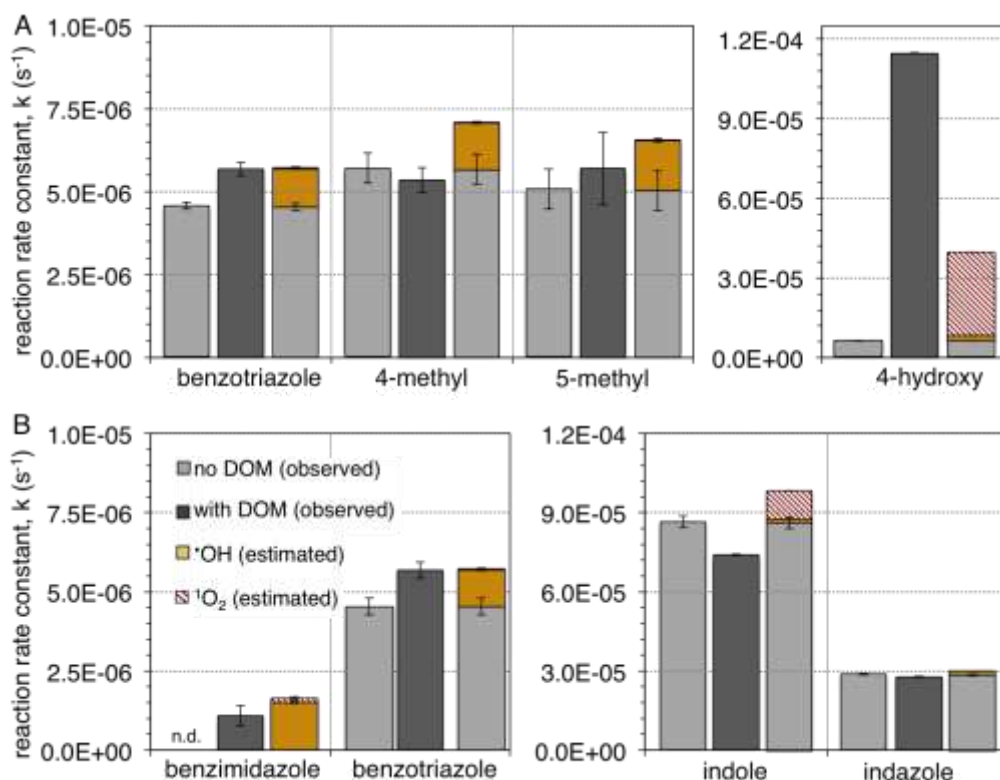
530 UVB light relative to organic matter concentration (Waskish Peat organic matter) as

531 observed (green filled diamonds) and corrected for light screening effects by the

532 organic matter (green open diamonds), lines connect data points. Measurements were

533 performed in duplicates (without SRFA) and triplicates (with SRFA).

534



535

536 **Figure 4.** Degradation rate constants, k (s⁻¹), for (A) benzotriazole derivatives and
 537 (B) structurally related compounds under simulated sunlight conditions observed for
 538 direct photochemical degradation without dissolved organic matter ('no DOM', light
 539 grey bars) and in the presence of DOM ('with DOM', dark grey bars, corrected for
 540 light screening by SRFA(II), 13 mg_C L⁻¹). Third stacked bars represent the expected
 541 degradation in the presence of DOM as the sum of direct and indirect photochemical
 542 processes. Indirect photochemical processes were estimated for the reaction with
 543 hydroxyl radical (yellow bars) and singlet oxygen (red striped bars) as the product of
 544 the compound specific reaction rate constants and steady-state concentrations of these
 545 reactive oxygen species. No degradation has been detected: n.d. Error bars represent
 546 one standard deviation.

547

548 **Table 1.** Reaction rate constants with singlet oxygen and hydroxyl radicals and direct
 549 and indirect photochemical half-lives during exposure to simulated sunlight and in the
 550 presence of dissolved organic matter (DOM) for benzotriazole derivatives and
 551 structurally related compounds.

Compound	Reaction rate constant k ($M^{-1} s^{-1}$)		Photochemical half-life $t_{1/2}$ (days)		
	hydroxyl radical ($\cdot OH$)	singlet oxygen (1O_2)	simulated sunlight		
			without DOM	with DOM ^a	$\cdot OH + ^1O_2$ ^b
Benzotriazole (BZ)	8.31 $\pm 0.13 \times 10^9$	$< 2.0 \times 10^5$	1.8	1.4	6.7
5-methyl BZ	8.81 $\pm 0.22 \times 10^9$	$< 6.2 \times 10^4$	1.4	1.5	5.6
4-methyl BZ	9.41 $\pm 0.34 \times 10^9$	$< 4.0 \times 10^4$	1.6	1.4	5.3
4-hydroxy BZ	12.20 $\pm 0.15 \times 10^9$	1.31 $\pm 0.04 \times 10^8$	1.3	0.1	0.2
Indole	8.94 $\pm 0.25 \times 10^9$	4.34 $\pm 0.01 \times 10^7$	0.1	0.1	0.7
Indazole	9.32 $\pm 0.16 \times 10^9$	$< 3.0 \times 10^5$	0.3	0.3	5.1
Benzimidazole	9.38 $\pm 0.17 \times 10^9$	$< 6.0 \times 10^5$	n.d.	7.4	4.9

552 ^a Suwannee River Fulvic Acid (II), 13 mg_C L⁻¹, ^b half-lives as the sum of the reaction
 553 with singlet oxygen and hydroxyl radical, estimated from the compound-specific
 554 reaction rate constant and steady-state concentrations for singlet oxygen (2.5×10^{-13}
 555 M) and hydroxyl radical (1.6×10^{-16} M).
 556